

DARK AND PHOTOCONDUCTIVITY OF CADMIUM-VANADIUM-SILVER OXIDE GLASSES

I. M. ASHRAF^{ab}, S. EL YOUSEF^{ac*}, S. ALMOEED^d

^aResearch Center for Advanced Materials Science (RCAMS), King Khalid University, Abha 61413, P. O. Box 9004, Saudi Arabia.

^bPhysics Dep., Faculty of Sciences, Aswan University, Aswan, Egypt.

^cPhysics Dep., Faculty of Science, Al- Azhar University, Assiut branch, Assiut, Egypt.

^dPhysics Dep., Faculty of College of Arts & Sciences King Khalid University, Muhail Asir, Saudi Arabia

Novel composition glasses such as $(V_2O_5)_{20}-(CdO)_{75}-(Ag_2O)_5$ in mol% have been prepared by a melting technique. The dark conductivity and photoconductivity, σ_{ph} , of these glasses at different of the intensity of light and various temperature were measured. The thermal stability structural and glassy phase investigated by using Raman spectroscopy, X-ray diffraction (XRD), scanning electron microscopy (SEM) and differential scanning calorimetric (DSC). These glasses has thermal stability $\Delta T = 97$ °C and anticrystallization parameter $S = 5.5$. The dark conductivity, σ , equal $6.39 \times 10^{-3} \Omega^{-1} \cdot cm^{-1}$ at 300 K, the value of photoconductivity, σ_{ph} , is $5.71 \times 10^{-3} \Omega^{-1} \cdot cm^{-1}$ at 4900 Lux with photosensitivity 0.89. The, σ_{ph} , value of the prepared glasses larger by comparing with other glass systems reported in the literature; hence it can be use in optoelectronic devices. Finally the structure of these glass investigated by using Raman spectra.

(Received August 1, 2017; Accepted November 6, 2017)

Keywords: Oxide glasses; photoconductivity; Raman; DSC

1. Introduction

Ionic oxide glasses are very important because of their have unique advantages like that high electric conductivity, low cost of preparation, a good thermal stability and the large different composition ranges which can used as potential candidates for electric application in batteries and sensors. Here the glasses contain $V_2O_5[(V^{4+}(3d^1) \text{ and } V^{5+})]$ are important due to use in memory switching devices and electrical threshold [1, 2]. Moreover, increase in importance of vanadate glasses are semiconductors at room temperature i.e their resistivity is low as $1 \Omega m$ depending on the ration of V_2O_5 content and the preparing conditions.

In the present work we added silver oxide to binary system V_2O_5 - CdO because Ag^+ is the fast ion conducting in the glasses matrix that behavior Ag^+ ion conducting of approximately $10^{-13} - 10^{-1} \Omega^{-1} \cdot cm^{-1}$ at room temperature [3- 5]. We can suggest that pure ionic conduction or pure electronic conduction and both electronic and ionic is expected in these glasses depending on melting condition and the composition of the glasses constituents with composition V_2O_5 - CdO- Ag_2O . This bulk glass that has mixed conduction mechanism can be candidate to use in optoelectronic devices hence, the aim of present paper we measure the dark, and the photoconductivity.

2. Experimental

*Corresponding authors: omn_yousef2000@yahoo.com

The glasses within the composition $(V_2O_5)_{20} - (CdO)_{75} - (Ag_2O)_5$ in mol% was prepared by melt quenching. Silica crucibles filled with powdered raw materials were placed in an electric furnace at $1200\text{ }^\circ\text{C}$ for 30 min in air. The melt which had a high viscosity was then cast on a stainless steel mold, subsequently; the sample was transferred to an annealing furnace and kept for 2 h at 430K . After that, the furnace was switched off, and the glass sample was allowed to cool. The calorimetric measurements of prepared glasses were carried out in Setaram (DSC 131 Evo). The prepared sample (15 mg) was sealed in an aluminum pan and it tempered at 10 K/min . An empty aluminum pan was used as a reference and in all cases flow of nitrogen was maintained at 40 ml/min in order to extract the gases emitted by the reaction, which are highly corrosive to the sensory equipment installed in the DSC 131 Evo furnace.

The samples were examined by X-ray diffraction, (Siemens D 6000) using CuK_α radiation at 40 kV in the 2θ range from 10 to 80° . For scanning electron microscopy with energy dispersion (SEM/EDX) a JEOL TM Model JSM-T330 operating at 25 kV was used. The sample was previously coated with gold (Au).

The sample used in the electric measurements was mounted on the cold finger inside a cryostat (LN Oxford DN1704-type), which was evacuated to about 10^{-4} Torr . An opaque, non-conducting mask with a slit of area $1\times 4\text{ mm}^2$ was placed over the sample to illuminate only the aforementioned area. There is a hole in the cold finger of the cryostat at which the non-conducting mask was placed, as shown in Fig. 1.

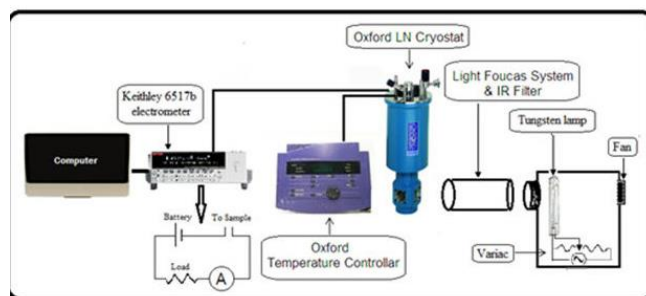


Fig. 1. Setup for measurements both dark conductivity and photoconductivity at different the light intensity and temperature

A digital temperature controller (Oxford ITC601-type) controlled the temperature inside the cryostat. The contacts between the samples and the metal electrodes were made using silver paste. The Ohmic behavior of the contacts was confirmed by the linear variations of the $I-V$ characteristic in the entire investigated voltage. Excitation was done by a tungsten lamp of 1000 W , which was connected to a variac for adjusting the light intensity at the sample surface. The adjustment was carried out for the longest distance between the light source and the sample with which enough clear spectral distribution can be obtained. Using an optical system consisting of two convex lenses, the light was focused onto the sample making sure that the region between the two electrodes was homogeneously illuminated. Proper care was taken to avoid the thermal effect of the light source, where the sample was mounted on the cold finger inside the evacuated cryostat (10^{-4} Torr). Moreover, the heat radiation from the light source was avoided by passing the light beam through a water filter. The measurement set up is equipped with a simple air cooling fan. In order to measure the dependency of the PC on the light intensity, the voltage applied to the light source was measured using a programmable digital electrometer (6517B Keithley Instrument). The net photocurrent was obtained by subtracting the dark current from the measured photocurrent. The total current (in the presence of light), at each point, was recorded after reaching a steady-state value. This value is often obtained 30 s later after such a change of illumination. A monochromator, of Carl Zeiss M4GII-type, was used for the dc-PC measurements. The vertical (VV) polarized

spontaneous Raman spectra of the prepared glass were acquired using a Thermo Scientific DXR Raman Microscope spectroscopy setup with 532 nm excitation [(532 nm Laser type Diode-pumped, solid state (DPSS)] and acquisition time was set to 30 seconds. The incoming signal vertically surface of the bulk sample, and V-polarized Raman scattered signal was collected in the backscattering geometry with a 100x microscope objective.

3. Results and discussion

The nature of the prepared sample with composition $(V_2O_5)_{20} - (CdO)_{75} - (Ag_2O)_5$ in mol% in mol% was confirmed from (XRD) and SEM. Figure (2a) show the XRD pattern for this sample do not show any sharp peaks caused by crystalline phases. Figure 2b depicted SEM images for the prepared glass, it show a glassy surface with no cluster of constitute oxide (V_2O_5 , CdO, Ag_2O). Furthermore the EDX analysis reveals that the Ag, V, Cd and O in present sample are free from contamination (see Fig. 2c).

Fig. (3) The thermal analysis of prepared glass to obtain glass transition temperature, T_g ; onset crystallization temperature, T_c ; thermal glass stability $\Delta T = (T_c - T_g)$; the peak of crystallization temperature, T_p and thermal stability of anticrystallization, S , determine as; $S = \frac{\Delta T \cdot (T_p - T_c)}{T_g}$. The results are summarized, $T_g = 467K$, $T_c = 564K$, $\Delta T = 97$ and $S = 5.5$, it is clear that these glass can resist thermal damage which has a suitable thermal stability and anti crystallization parameters.

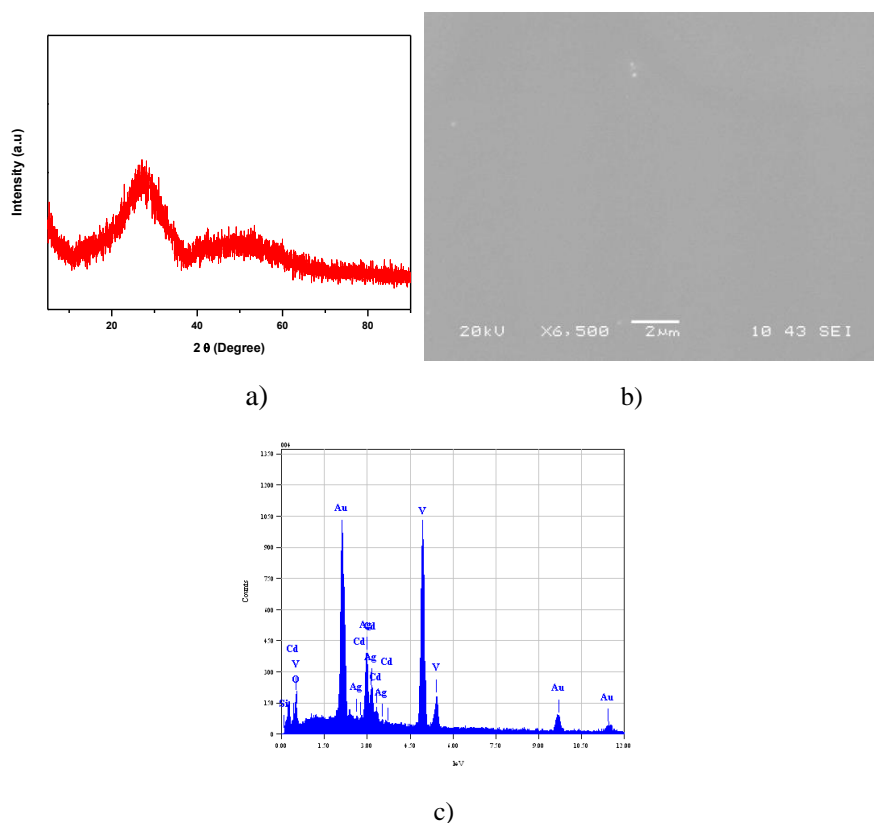


Fig.2a, b, c: XRD-pattern, SEM and EDX of the prepared glass with the composition $(V_2O_5)_{20}(CdO)_{75}(Ag_2O)_5$ in mol%.

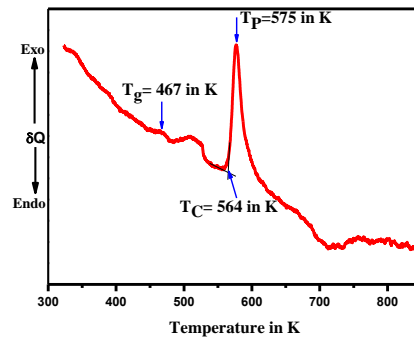


Fig. 3. DSC profile of present glasses $(V_2O_5)_{20}(CdO)_{75}(Ag_2O)_5$ in mol%

The dependence of temperature on dark electrical (σ) and photo conductivity (σ_{ph}) was studied at different levels of white light intensities (600, 2750 and 4900 Lux) as shown in figure (4). From these figure it is evident that the conductivity increases linearly with temperature in the range from 295 K to 400 K, which indicates that the conduction in this range has single activation energy. The exponential behavior of electrical and photo conductivity is described by the following equation:

$$\sigma = \sigma_0 \cdot \exp \left[\frac{-E_a}{K_B T} \right] \quad (1)$$

Where, σ_0 and E_a are denote that the pre-exponential factor and the activation energy respectively.

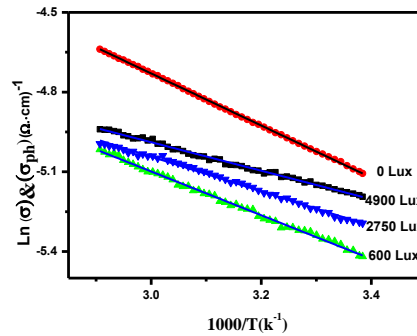


Fig. 4. The dark, σ , and photoconductivity, σ_{ph} , at different light intensity.

By comparing our result with other results reported of different glasses systems such as; glasses Se-Te-Pb ($\sigma_{ph}=1.11 \times 10^{-4} \Omega^{-1} \cdot \text{cm}^{-1}$ and $\sigma_d=5.56 \times 10^{-4} \Omega^{-1} \cdot \text{cm}^{-1}$) [6]; Se-Ge-Ag glasses has ($\sigma_{ph}= 6.07 \times 10^{-8} \Omega^{-1} \cdot \text{cm}^{-1}$ and $\sigma_d=7.89 \times 10^{-8} \Omega^{-1} \cdot \text{cm}^{-1}$) [7]; Se-Te-Ge glass ($\sigma_{ph}= 3.57 \times 10^{-7} \Omega^{-1} \cdot \text{cm}^{-1}$ and the $\sigma_d = 2.46 \times 10^{-6} \Omega^{-1} \cdot \text{cm}^{-1}$) [8] and $\sigma_{ph} = 1.97 \times 10^{-7}$ and $\sigma_d = 2 \times 10^{-8} \Omega^{-1} \cdot \text{cm}^{-1}$ were reported for Ge-Se-Sn glasses [9]. In the present work it is note that the σ_{ph} value of present glasses are larger than compared with glasses were reported in Ref. [6- 9].

The activation energy (E_a) and the pre-exponential factor (σ_0) were calculated from the slope and the intercepts of the figure lines at different light intensities, and they are given in table 1.

It is noted from the results that the activation energy of oxide glass ceramics $(V_2O_5)_{20}(CdO)_{75}(Ag_2O)_5$ decreases with increasing the intensity of light. This behavior is due to the shift of Fermi level with increasing the light intensity. The results showed a exponential correlation between the pre-exponential factors (σ_0) and the activation energy (E_a). Figure (5) shows this correlation $\ln \sigma_0$ versus E_a , it was found to be linear relationship. This behavior is known as Meyer-Neldel Factor (MNF) [10, 11], and it has already been observed in the many amorphous materials and glassy alloy [12, 13]. The following equation (2) describes this behavior:

$$\sigma_0 = \sigma_{00} \cdot \exp[E/K_B \cdot T_0] \quad (2)$$

Where, σ_{00} (M.N.F) and it is equal $4.8 \times 10^{-3} (\Omega \cdot \text{cm})^{-1}$ also $(K_B T_0)^{-1}$ is Meyer Nelded Characteristic Energy (MNCE) it is computed $20.36 (\text{eV})^{-1}$.

By using the calculated values, σ_0 , and compared with the values which calculated from equation (1), the values were found to be close together (see table 1).

Table 1. Obtain the dark conductivity, σ , and photoconductivity, σ_{ph} , Meyer-Neldel Factor (MNF), σ_{00} , activation energy and photosensitivity, S , of present glasses

Intensities (Lux)	$\sigma(\Omega \cdot \text{cm})^{-1}$ at 300K	$\sigma_0(\Omega \cdot \text{cm})^{-1}$	Calculated values of $\sigma_{00}(\Omega \cdot \text{cm})^{-1}$	$E_a(\text{eV})$	Photo Sensitivity, S , (at 300K)
0	6.39×10^{-3}	16.72×10^{-2}	14.96×10^{-2}	0.169	0.0
600	4.69×10^{-3}	7.23×10^{-2}	8.63×10^{-2}	0.142	0.73
2750	5.14×10^{-3}	4.57×10^{-2}	4.69×10^{-2}	0.112	0.81
4900	5.71×10^{-3}	3.41×10^{-2}	3.12×10^{-2}	0.092	0.89

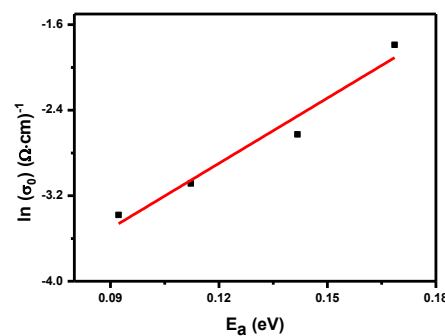


Fig.5. Show, $\ln \sigma_0$ versus E_a , of prepared glasses.

The important parameter in the photoconductivity strides is the photosensitivity, where it determines the application of the material in the photoconductive devices [10]. The photosensitivity is determined in the room temperature by the relation:

$$S = \sigma_{ph}/\sigma_d \quad (3)$$

The values of photosensitivity at different light intensities are listed in table 1. It is observed from the table that the photoconductivity and photosensitivity increase with increasing light intensity, which could be due to the generation of more number of free charge carriers.

The photocurrent has been plotted as a function of light intensity for classification our compound with respect to the types of the recombination as shown in figure 6. Since the relation between the photocurrent and light intensity obeys the power law:

$$I_{ph} \propto F^\gamma \tag{4}$$

Where γ is a constant and its value determines the recombination process. In our investigation, the value of γ was found to be 0.63, which suggested that; there are impure state (traps state) distributed in the energy gap [14]. The recombination and trapping mechanism can be understood using transient photoconductivity study [15]. The transient photoconductivity was investigated at different light intensities (289, 1740, 3640, and 6100 Lux) and different temperatures (298– 400K) at constant applied voltage (0.5 volt) by studying the dependence of the photocurrent on time during the process of lighting (a, b region) and darkness (c,d region) as seen in figures (6 and 7).

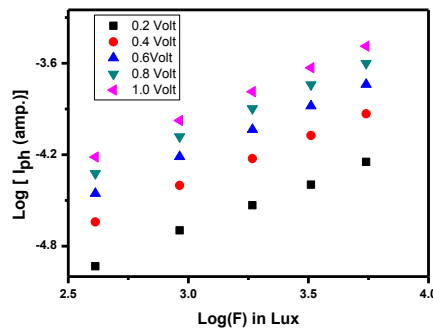


Fig. 6: Show that relation between $\log(I_{ph})$ in amp and $\log(F)$ in Lux.

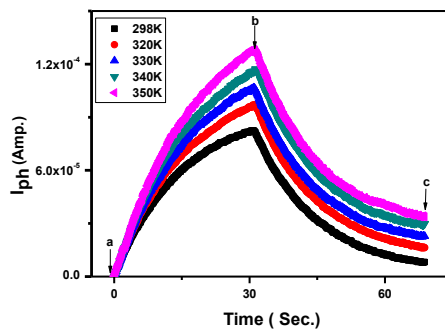


Fig. 7: Dependence of the photocurrent on time during the process of lighting (a, b region) and darkness (c, d region).

These figures show that the growth and decay curves having non-exponential behaviors, which indicates that there are traps in the oxide glass ceramics $(V_2O_5)_{20}(CdO)_{75}(Ag_2O)_5$. At the beginning of the curve the photocurrent rises with a fast rate due to the generation of

photo-carriers, and then it becomes slower due to the trap filling. After blocking the light from the sample; the decay starts rapidly due to the recombination process and then the traps emptying makes it to be slower [16]. The rate of traps filling during current rises or traps emptying during decay depends on their cross sections and ionization energy [17]. The presences of traps make the carrier lifetime to be longer. So, the carrier lifetime can be expressed by differential lifetime concept [18].

$$\tau_d = - \left[\frac{1}{I_{ph}(\max)} \cdot \frac{dJ_{ph}(t)}{dt} \right] \left[\frac{1}{I_{ph}(\max)} \cdot \frac{dJ_{ph}(t)}{dt} \right]^{-1} \quad (5)$$

Where $\frac{dI_{ph}(t)}{dt}$ is the decay rate and can be calculated from the current decay region and $I_{ph}(\max)$ is the saturated value of photocurrent. Figure 8 shows the differential lifetime dependence on time at different temperatures. It is obtained that the differential lifetime increases with time indicating that the band gap has a continuous distribution of defect states [18-20]. The results showed increasing of differential lifetime values with temperature increase, which indicates the dependence of the differential life time on the temperature. The response time is determined as during the photocurrent rises or decays into $1/e$ of its steady state value after turning on or off the light [14]. The dependence of differential lifetime at response time at different light intensity is show in figure (9), the differential lifetime at response time is reversely dependent on the light intensity. This is may be due to the probability of trapping process increases with increasing the light intensity [14].

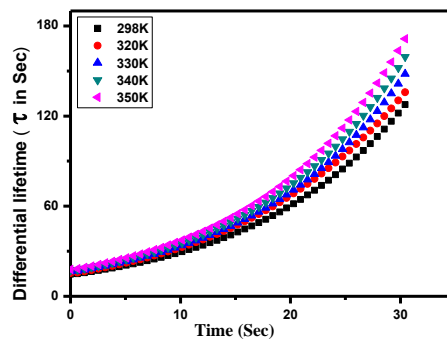


Fig. 8: Shows the differential lifetime dependence on time at different temperatures.

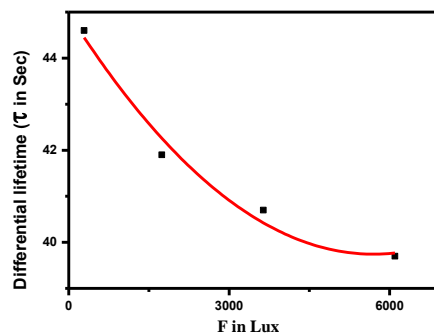


Fig. 9: Obtain that dependence of differential lifetime at response time at different light intensity.

Figure (10) obtain the Raman spectra of glass $(V_2O_5)_{20} - (CdO)_{75} - (Ag_2O)_5$ in mol% were excited with a power of $\approx 0.1mW$ by using DPSS at wave number ($\nu_l=1.880 \times 10^4$ in cm^{-1}). Raman spectra deconvolution to seven peaks at 58, 142, 260, 504, 688, 760 and 970 cm^{-1} are designated. In the binary system CdO- V_2O_5 was achieved when the bridges V-O-V in the $[V_2O_7]^{4-}$ anions of $Cd_2V_2O_7$ are broken by excessive insertion of Cd^{2+} ions with higher CdO content. It assumed that in the present amorphous material contains a disorder network that includes VO_3 and VO_4 units which are the basic components of the compounds $Cd_2V_2O_7$. The structure of V_2O_5 as former in the vanadate glass has different phase as follow; (1) VO_4 and VO_5 units, (2) pyrovanadates as a form $M_2V_2O_7$, (3) metavanadate groups MV_2O_6 or $M(VO_3)_2$ where M is metal ions [20, 21].

Herein it is found that very strong peak with a maximum at $58cm^{-1}$ is identified with the Boson peak which a characteristic feature of a glassy phase of prepared sample. We could be supposed that Ag and Cd ions take place in the inter layers of the VO_4 units, this means that Cd atoms that reside in the structure of the V_2O_5 layers. The bands centered around 142, 250 and 504 cm^{-1} , they may be related to CdO and Ag_2O compound. At high concentration of CdO (70 mol%) in the prepared glasses V_2O_5 - CdO- Ag_2O , the VO_3 units linked through bridges V-O-V in the $[V_2O_7]^{4-}$ anions of $Cd_2V_2O_7$ are formed when the bridge V-O-V broken, hence release Cd^{2+} ions leads to increase the conductivity of present glass. So in the Raman spectra the band at 820 cm^{-1} disappears it related to V-O-V (see Fig. 9). Maybe this glass formed by a combination of disordered network that main contains VO_3 and VO_4 units. Where the Raman scattering for units occurs at 688 cm^{-1} related to VO_3 assume that, it was released from $[V_2O_7]^{4-}$ anions of $Cd_2V_2O_7$ phase and the highest frequency at 760 cm^{-1} the VO_4 units were occurred. The band at 980 cm^{-1} is attributed to the stretching modes of V=O terminal bond.

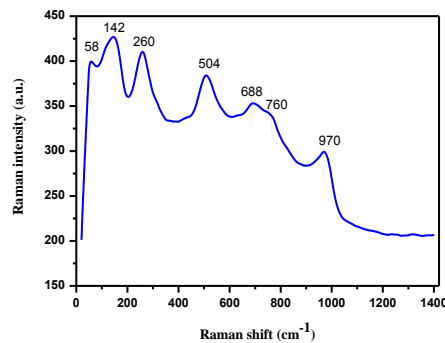


Fig. 10: Raman spectra of present glasses with composition $(V_2O_5)_{20} - (CdO)_{75} - (Ag_2O)_5$ in mol%.

4. Conclusions

In the present work photo and dark conductivity measurements were performed in the glass with composition $(V_2O_5)_{20} (CdO)_{75} (Ag_2O)_5$. Incorporation of CdO with high concentration into the binary system V_2O_5 - Ag_2O leads to these glasses has a suitable thermal stability $\Delta T= 97$ °C, anticrystallization parameter $S= 5.5$ and high value of photoconductivity, σ_{ph} , is $5.71 \times 10^{-3} \Omega^{-1} \cdot cm^{-1}$ at 4900 lux. At high concentration of CdO (70 mol%) in the prepared glasses V_2O_5 - CdO- Ag_2O

creation the VO_3 units linked through bridges V-O-V in the $[\text{V}_2\text{O}_7]^{4-}$ anions of $\text{Cd}_2\text{V}_2\text{O}_7$ are formed when the bridge V-O-V broken, hence release Cd^{2+} ions leads to increase the conductivity.

Acknowledgements

The authors would like to express their gratitude to Research Center of Advanced Materials- King Khalid University, Saudi Arabia for support.

References

- [1] A. Ghosh J. Appl. Phys. **64**,2652 (1988).
- [2] G. Govindaraj, N. Baskaran, K. Shahi, P. Monoravi, Solid State Ionic **76**,47 (1995).
- [3] C. A. Angell, Annu. Rev. Phys. Chem. **43**,693 (1992).
- [4] T. Minami, J. Non-Cryst. Solids **56**,15 (1983).
- [5] W. Martin J. Am. Ceram. Soc. **74**, 1767 (1991).
- [6] N. Kushwaha, V. S. Kushwaha, R. K. Shukla, A. Kumar, J. Non. Cryst. Solids **351**,3414 (2005).
- [7] I M Ashraf, M M Abdel-Rahman and A M Badr, Journal of Physics D: Applied Physics **36**(2),(2002).
- [8] I. M. Ashraf, H. A. El-Shaikh and A. M. Badr, PRAMANA journal of physics **68**,467 (2007).
- [9] I. M. Ashraf, H. A. Elshaikh , A. M. Badr,phys. stat. sol. (b)**241**(4), 885 (2004).
- [10] I. M. Ashraf, H. A. Elshaikh , A. M. Badr,Cryst. Res. Technol. **39**(1), 63 (2004).
- [11] D. Kumar, S. Kumar, Turk J. Phys. **29**,91 (2005).
- [12] A. Thakur, V. Sharma, P. S. Chandel, N. Goyal, G. S. S. Sani, S. K. Tripathi, J. Mater Sci. **41**,2327 (2006).
- [13] Qiu Fen, Xiang Jinzhon, Kong Jincheng, Yu Lianjie, Kong Lingde, Wang Guanghua, Li Xiongju, Yang Lili, Li Cong, and Ji Rongbin, Journal of Semiconductors**32**(3),1 (2011).
- [14] Dwivedi, M.Dixit, and Kumar, Journal of materials science letters**17**, 233 (1998).
- [15]S. Singh, R. S. Sharma, R. K. Shukla, A. Kumar, Chalcogenide Letters **1**(7), 83 (2004).
- [16]D.Kumar, S.Kumar, Chalcogenidel letters **16**(6), 79 (2004)
- [17] A. S. Maan, D. R. Goyal and A. Kumar, Revue Phys. Appl.**24**,613 (1989).
- [18]W. Fuhs and J. Stuke , Physics Status Solidi, **27**,171 (1968).
- [19] R.H. Bube, photoconductivity of solids. New York: Wiley, (1978).
- [20]Gillian Althea Maria Reynolds, Electronic Transport and Photoconductive Properties of Resorcinol-Formaldehyde-Based Carbon Aerogels, (1989).
- [21] R. Lozada Morales, A. Cid-Garxia, E. Cervantes Juarez, J. Ma Eincon, G. Lopez-Calzada, J. Carmona-Rodriguez, Ma. E. Zayas, O. Zelaya-Angel, S. Jimenez-Sandoval, J. Non-Cryst. Solids **398&399**,10 (2014).
- [22] Ponnada Tejeswara Rao, Kocharlakota V. Ramesh, Devulapalli L. Sastry, New J. of Glass and Ceramics**2**,34 (2012).